Supplemental information

Inositol serves as a natural inhibitor of mitochondrial fission by directly targeting AMPK

Che-Chia Hsu, Xian Zhang, Guihua Wang, Weina Zhang, Zhen Cai, Bo-Syong Pan, Haiwei Gu, Chuan Xu, Guoxiang Jin, Xiangshang Xu, Rajesh Kumar Manne, Yan Jin, Wei Yan, Jingwei Shao, Tingjin Chen, Emily Lin, Amit Ketkar, Robert Eoff, Zhi-Gang Xu, Zhong-Zhu Chen, Hong-Yu Li, Hui-Kuan Lin

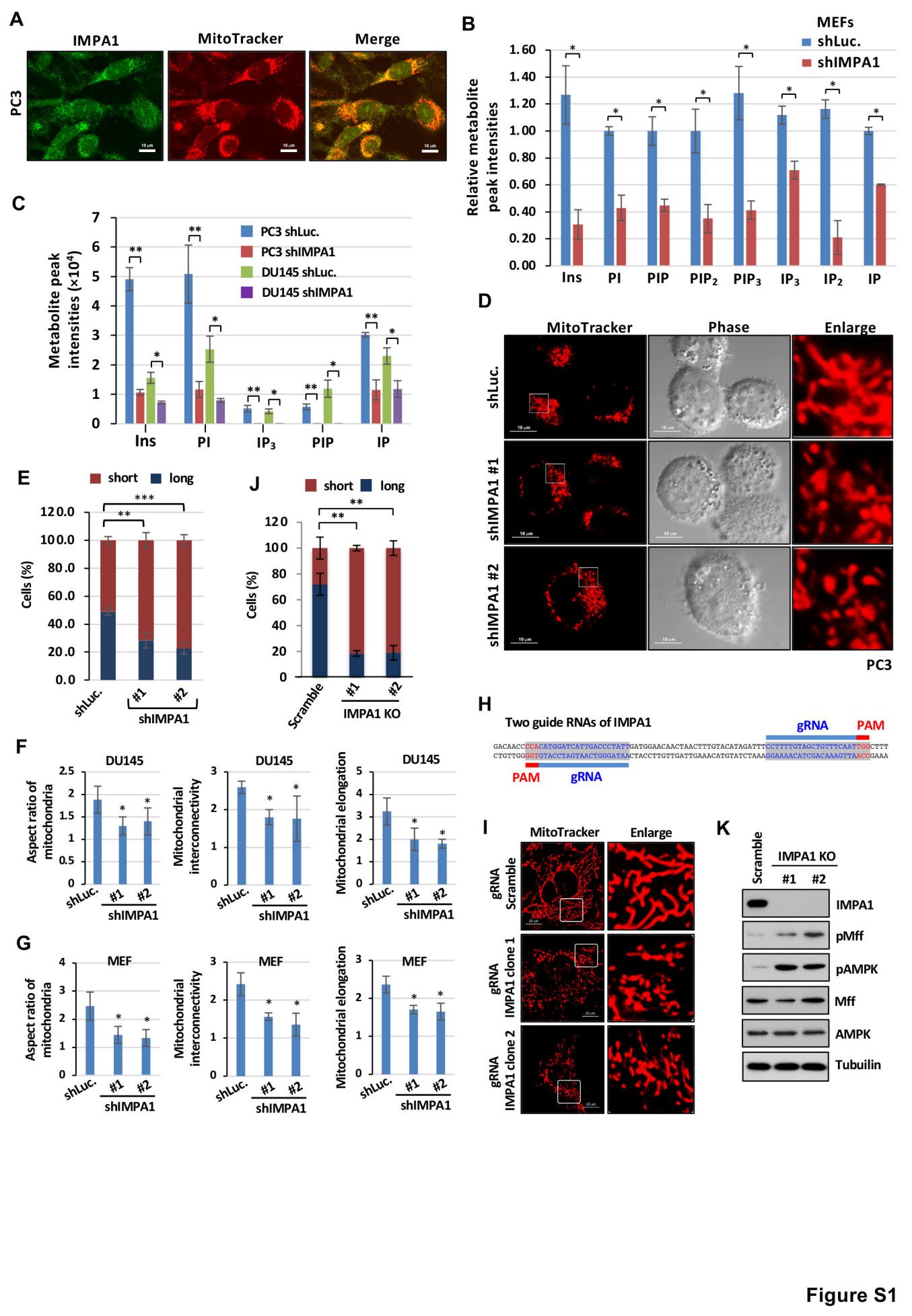
A
IMPA1
MitoTracker
Merge
PC3
B
MEFs
shLuc.
shIMPA1
Relative metabolite peak intensities
Ins
PI
PIP
PIP2
PIP3
IP3
IP2
IP
C
PC3 shLuc.
PC3 shIMPA1
DU145 shLuc.
DU145 shIMPA1
Metabolite peak intensities (×10⁴)
D
MitoTracker
Phase
Enlarge
shLuc.
shIMPA1 #1
shIMPA1 #2
PC3
E
short
long
Cells (%)
shLuc.
#1
#2
shIMPA1
J
Scramble
IMPA1 KO
F
DU145
Aspect ratio of mitochondria
Mitochondrial interconnectivity
Mitochondrial elongation
G
MEF
H
Two guide RNAs of IMPA1
gRNA
PAM
I
MitoTracker
Enlarge
gRNA Scramble
gRNA IMPA1 clone 1
gRNA IMPA1 clone 2
K
Scramble
IMPA1 KO
IMPA1
pMff
pAMPK
Mff
AMPK
Tubulin

Figure S1

Figure S1. IMPA1/2-derived Inositol inhibits mitochondrial fission, Related to Figure 1.

(A) Confocal images of subcellular localization of IMPA1 by specific IMPA1 antibody in PC3. (B) Metabolic profiling MEFs expressing shLuc. or shIMPA1 was performed by targeted mass spectrometry analysis of phosphoinositides metabolism. (C) Metabolic profiling of PC3 or DU145 cells expressing shLuc. or shIMPA1 was performed by targeted mass spectrometry analysis of phosphoinositides metabolism. (D) Confocal images of mitochondrial morphology in PC3 cells stably transduced with shLuc. or shIMPA1. Scale bar, 10 μm in MitoTracker. (E) Quantification of the mitochondrial morphology of PC3 cells shown in (D). Data are shown as the mean ± SEM of three independent experiments with 100 cells counted for each replicate. (F) Graphic respectively represents individual mitochondrial aspects ratio, interconnectivity and elongation in DU145 cells expressing shLuc. or shIMPA1 after quantitative image analysis. Y axis of mitochondrial aspects ratio, interconnectivity and elongation is arbitrary unit. (G) Mitochondrial aspects ratio, interconnectivity and elongation in MEFs expressing shLuc. or shIMPA1 (#1 and #2) after quantitative image analysis. (H) Illustration of cDNA sequence of IMPA1 targeted by the guide RNA pairs for IMPA1 knockout by CRISPR/Cas9. (I) Confocal images with MitoTracker (Red) in DU145 cells stably transduced with the guide RNA pairs of scramble or IMPA1 (#1 and #2). (J) Quantification of the mitochondrial morphology of the cells shown in (I). (K) Immunoblotting of CRISPR/Cas9 knockout cells transduced with the guide RNA pairs of scramble or IMPA1 including two single clones (#1 and #2).

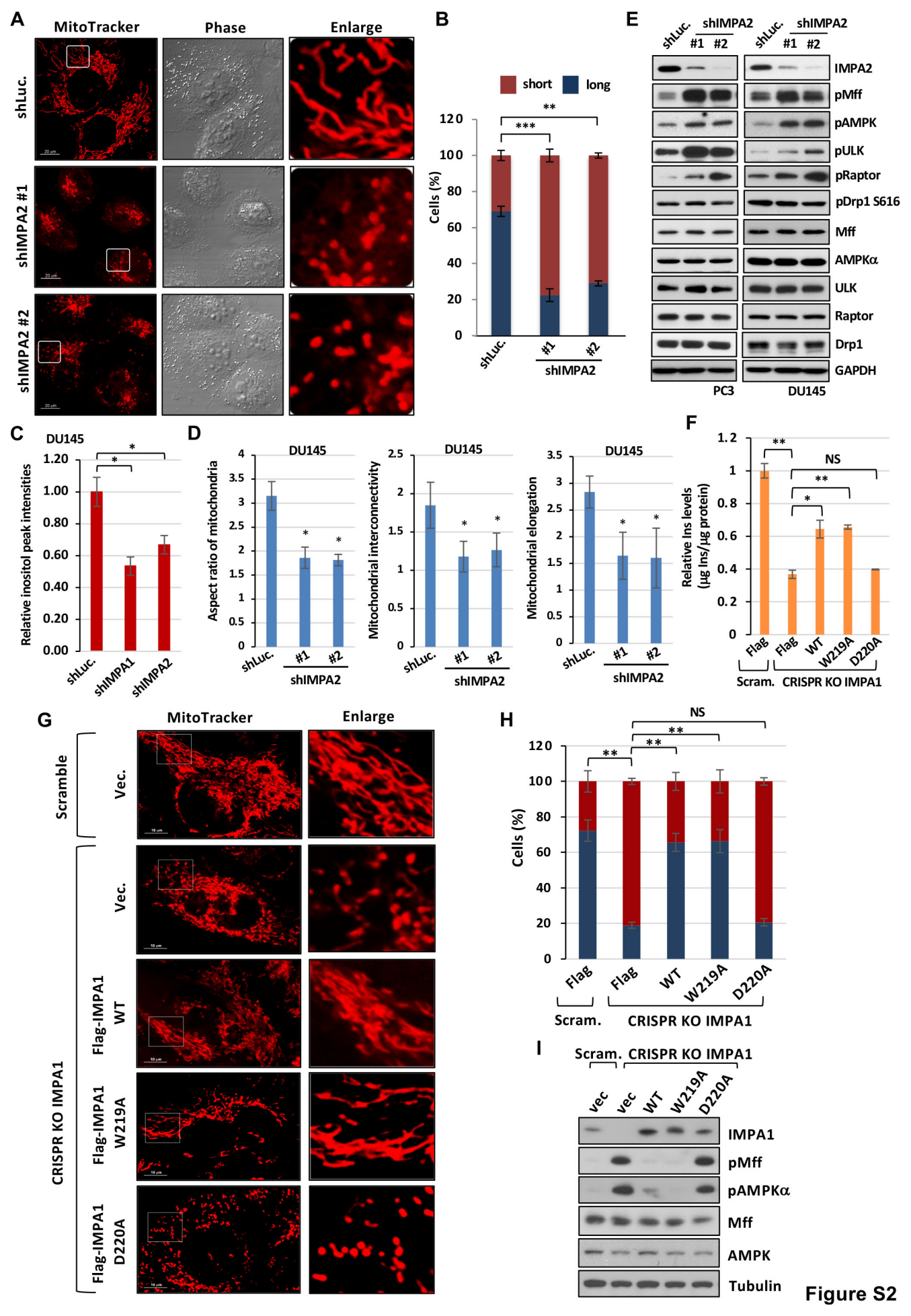
A
MitoTracker
Phase
Enlarge
shLuc.
shIMPA2 #1
shIMPA2 #2
B
short
long
Cells (%)
shLuc.
#1
#2
shIMPA2
E
shLuc.
shIMPA2
#1
#2
IMPA2
pMff
pAMPK
pULK
pRaptor
pDrp1 S616
Mff
AMPKα
ULK
Raptor
Drp1
GAPDH
PC3
DU145
C
DU145
Relative inositol peak intensities
shLuc.
shIMPA1
shIMPA2
D
DU145
Aspect ratio of mitochondria
Mitochondrial interconnectivity
Mitochondrial elongation
F
Relative Ins levels (μg Ins/μg protein)
NS
Flag
WT
W219A
D220A
Scram.
CRISPR KO IMPA1
G
MitoTracker
Enlarge
Scramble
Vec.
CRISPR KO IMPA1
Flag-IMPA1 WT
Flag-IMPA1 W219A
Flag-IMPA1 D220A
H
Cells (%)
NS
Flag
WT
W219A
D220A
Scram.
CRISPR KO IMPA1
I
Scram.
CRISPR KO IMPA1
vec
WT
W219A
D220A
IMPA1
pMff
pAMPKα
Mff
AMPK
Tubulin

Figure S2

Figure S2. Restoration of inositol rescues aberrant mitochondrial fission upon IMPA loss, Related to Figure 2.

(A) Confocal images in DU145 cells stably transduced with shLuc. or shIMPA2. Scale bar, 20 μm. (B) Quantification of the mitochondrial morphology of the DU145 cells shown in (A). (C) Metabolic profiling of inositol in DU145 cells expressing shLuc., shIMPA1 and shIMPA2 was performed. (D) Graphic respectively represents individual mitochondrial aspects ratio, interconnectivity and elongation in DU145 cells expressing shLuc. or shIMPA2 after quantitative image analysis. (E) Immunoblotting of the PC3 or DU145 cells stably transduced shLuc. or shIMPA2. (F) The levels of inositol in DU145 scramble (Scram.) or IMPA1 knockout by CRISPR/Cas9 cells upon indicated plasmid overexpression were determined by K-INOSL assay kit. (G) Confocal images in DU145 scramble (Scram.) or IMPA1 knockout by CRISPR/Cas9 cells upon indicated plasmid overexpression. Scale bar, 10 μm. (H) Quantification of the mitochondrial morphology of the DU145 cells shown in (G). (I) Immunoblotting of CRISPR/Cas9 knockout cells transduced with the guide RNA pairs of scramble or IMPA1 upon indicated plasmid overexpression with indicated antibodies.

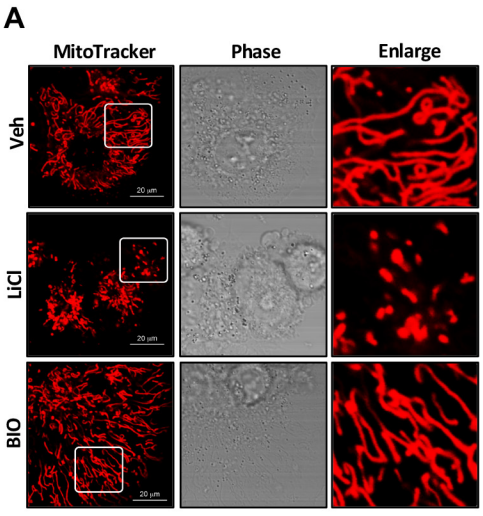

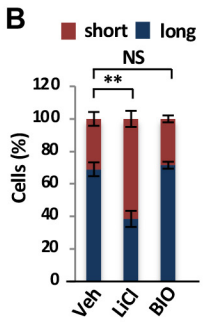

D

	PC3	22RV1	TRAMP-C2	MEFs	Kindney	Serum
Mean	786.00	963.23	962.77	394.60	641.67	179.41
SD	132.94	14.47	27.19	9.05	16.50	0.83

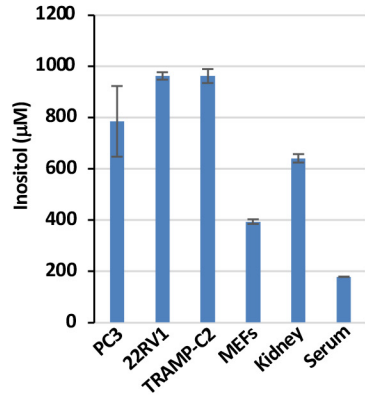

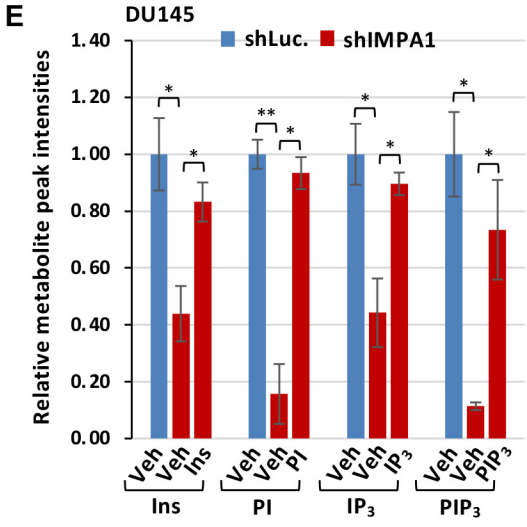

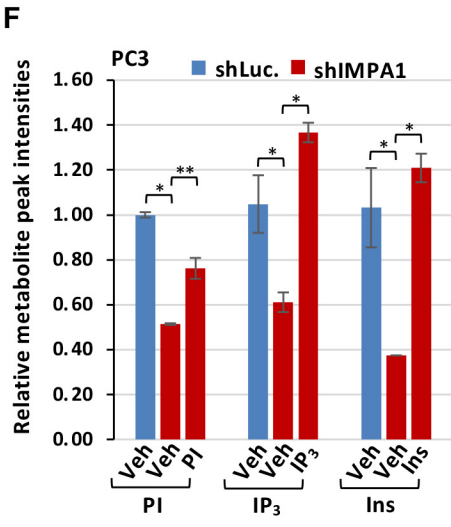

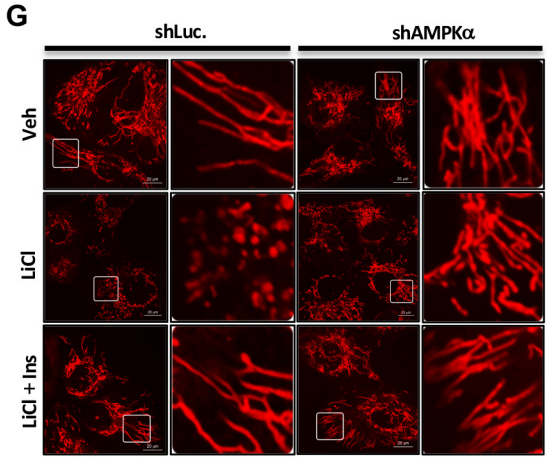

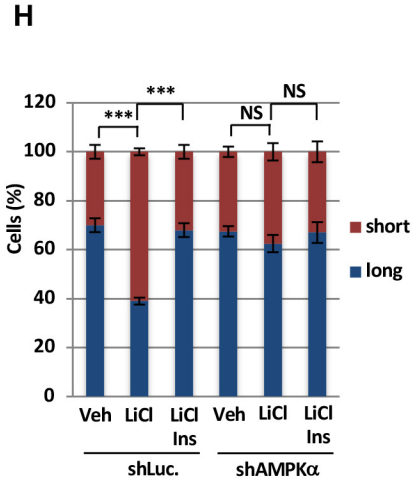

Figure S3

Figure S3. Restoration of inositol rescues aberrant mitochondrial fission upon IMPA inhibition by lithium chloride, Related to Figure 2.

(A) Representative confocal images by MitoTracker upon 500 μM of lithium chloride (LiCl) or 10 μM of BIO treatment for 30 minutes in DU145 cells. Veh, vehicle. (B) Quantification of the mitochondrial morphology of the cells shown in (A). Colors indicate the mitochondrial morphology (long or short). (C) Immunoblotting of DU145 cells upon vehicle (Veh), 500 μM of lithium chloride (LiCl) or 10 μM of BIO treatment. (D) The physiological concentration of inositol in diverse cells, mouse kidney and serum were determined. Three male mice were analyzed in each group. (E and F) Metabolic profiling of Ins, PI, IP_3 or PIP_3 in DU145 or PC3 cells expressing shIMPA1 upon vehicle (Veh), 25 μM of inositol (Ins), 4 μM of phosphatidylinositol (PI), inositol trisphosphate (IP_3) or phosphatidylinositol 3,4,5-bisphosphate (PIP_3) treatment was performed. (G) Representative confocal images in DU145 cells stably expressing shLuc. or shAMPKα (#1) upon non-treatment (NT), 500 μM of LiCl or 500 μM of LiCl plus Ins treatment for 30 minutes. Scale bar, 20 μm. (H) Quantification of the mitochondrial morphology of the cells shown in (G). Colors indicate the mitochondrial morphology (long or short).

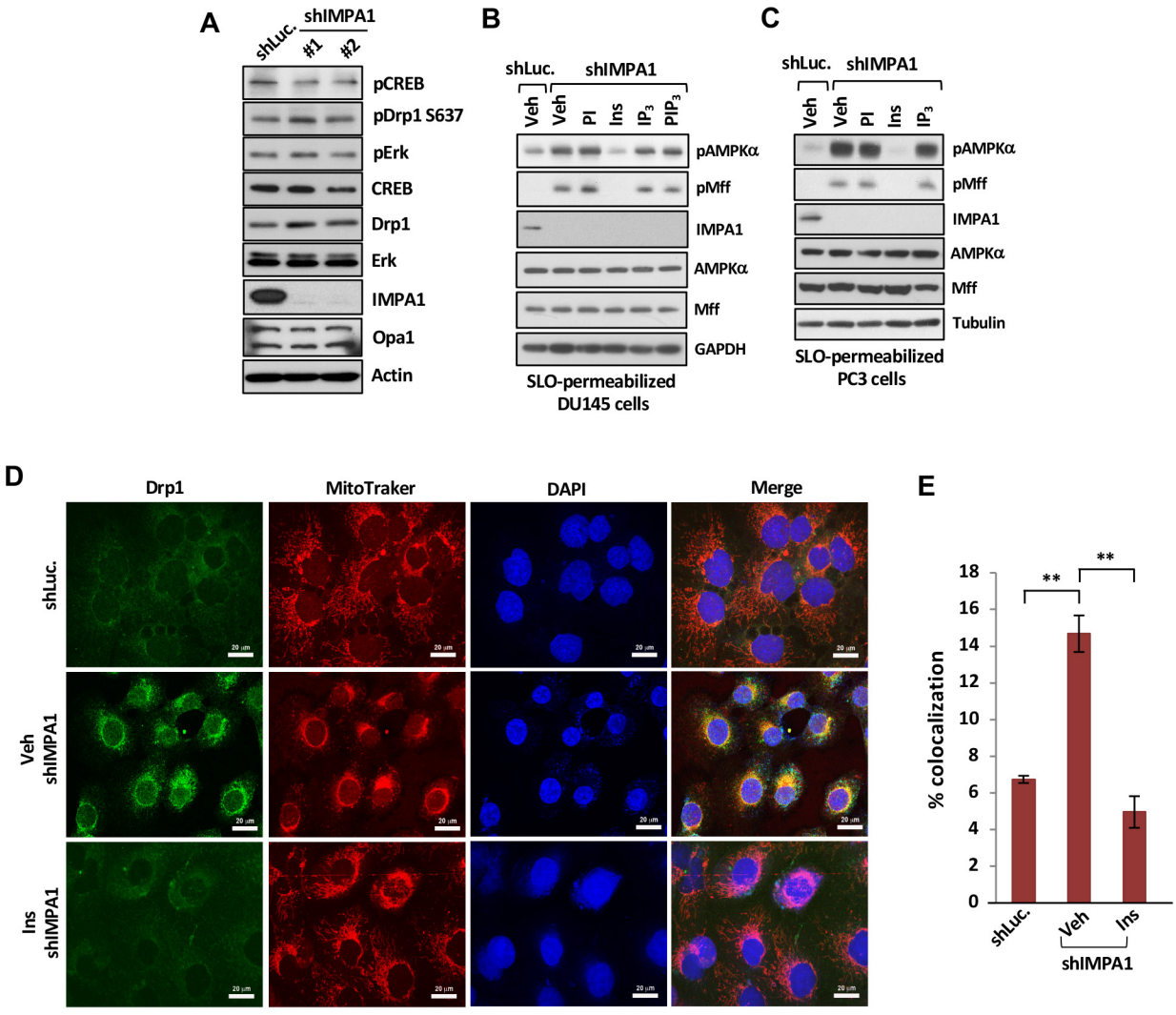
A
shLuc.
shIMPA1
#1
#2
pCREB
pDrp1 S637
pErk
CREB
Drp1
Erk
IMPA1
Opa1
Actin
B
shLuc.
shIMPA1
Veh
Veh
PI
Ins
IP3
PIP3
pAMPKα
pMff
IMPA1
AMPKα
Mff
GAPDH
SLO-permeabilized
DU145 cells
C
shLuc.
shIMPA1
Veh
Veh
PI
Ins
IP3
pAMPKα
pMff
IMPA1
AMPKα
Mff
Tubulin
SLO-permeabilized
PC3 cells
D
Drp1
MitoTraker
DAPI
Merge
shLuc.
Veh shIMPA1
Ins shIMPA1
20 μm
E
% colocalization
18
16
14
12
10
8
6
4
2
0
**
**
shLuc.
Veh
Ins
shIMPA1

Figure S4

Figure S4. Restoration of inositol rescues aberrant mitochondrial fission upon IMPA knockdown independently of its intermediates of phosphatidylinositol cycle, Related to Figure 2. (A) Immunoblotting of PC3 cells stably transduced with shLuc. or IMPA1-two specific shRNAs. (B and C) Immunoblotting of DU145 or PC3 cells stably expressing shLuc. or shIMPA1 preincubated with streptolysin O (SLO) for 5 minutes upon Ins, PI, IP_3 or PIP_3 treatment for 15 minutes. (D) Representative confocal images of DU145 cells stably transduced with shLuc. or shIMPA1 upon vehicle (Veh) or Ins treatment for 24 hours stained by MitoTracker Red FM (red) and Drp1 antibody (green). Scale bar, 20 μm. (E) Quantification of colocalization of MitoTracker and Drp1 by ImageJ. Representative immunoblotting blots for each dataset were presented from at least three times of the repeated experiments.

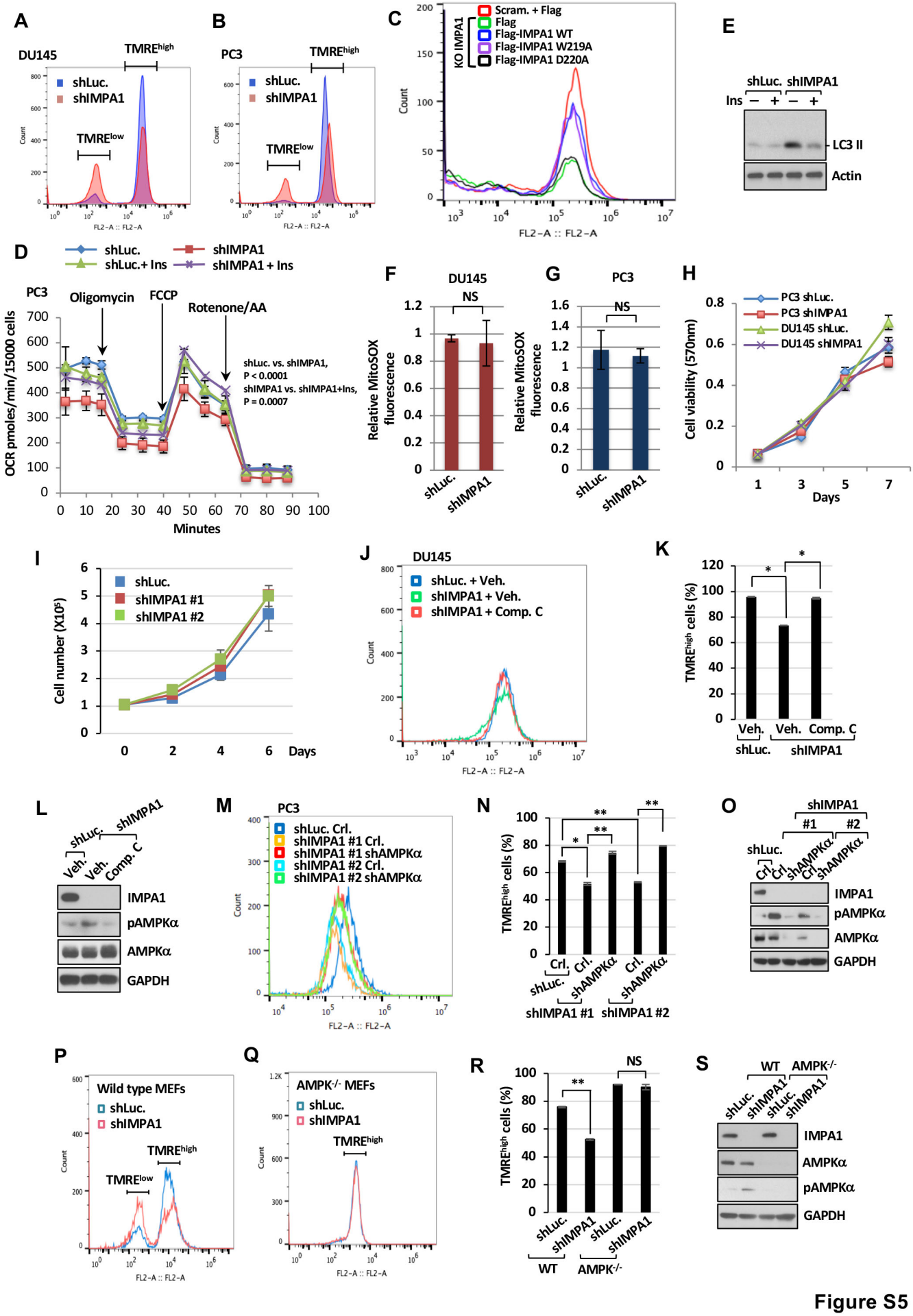
A
DU145
TMRE^high
shLuc.
shIMPA1
TMRE^low
Count
FL2-A :: FL2-A
B
PC3
TMRE^high
shLuc.
shIMPA1
TMRE^low
Count
FL2-A :: FL2-A
C
KO IMPA1
Scram. + Flag
Flag
Flag-IMPA1 WT
Flag-IMPA1 W219A
Flag-IMPA1 D220A
Count
FL2-A :: FL2-A
E
shLuc.
shIMPA1
Ins
LC3 II
Actin
D
shLuc.
shLuc.+ Ins
shIMPA1
shIMPA1 + Ins
PC3
Oligomycin
FCCP
Rotenone/AA
shLuc. vs. shIMPA1, P < 0.0001
shIMPA1 vs. shIMPA1+Ins, P = 0.0007
OCR pmoles/min/15000 cells
Minutes
F
DU145
NS
Relative MitoSOX fluorescence
shLuc.
shIMPA1
G
PC3
NS
Relative MitoSOX fluorescence
shLuc.
shIMPA1
H
PC3 shLuc.
PC3 shIMPA1
DU145 shLuc.
DU145 shIMPA1
Cell viability (570nm)
Days
I
shLuc.
shIMPA1 #1
shIMPA1 #2
Cell number (X10^5)
Days
J
DU145
shLuc. + Veh.
shIMPA1 + Veh.
shIMPA1 + Comp. C
Count
FL2-A :: FL2-A
K
TMRE^high cells (%)
Veh.
Veh.
Comp. C
shLuc.
shIMPA1
L
shLuc.
shIMPA1
Veh.
Veh.
Comp. C
IMPA1
pAMPKα
AMPKα
GAPDH
M
PC3
shLuc. Crl.
shIMPA1 #1 Crl.
shIMPA1 #1 shAMPKα
shIMPA1 #2 Crl.
shIMPA1 #2 shAMPKα
Count
FL2-A :: FL2-A
N
TMRE^high cells (%)
Crl.
Crl.
shAMPKα
Crl.
shAMPKα
shLuc.
shIMPA1 #1
shIMPA1 #2
O
shIMPA1
#1
#2
shLuc.
Crl.
Crl.
shAMPKα
Crl.
shAMPKα
IMPA1
pAMPKα
AMPKα
GAPDH
P
Wild type MEFs
shLuc.
shIMPA1
TMRE^high
TMRE^low
Count
FL2-A :: FL2-A
Q
AMPK-/- MEFs
shLuc.
shIMPA1
TMRE^high
Count
FL2-A :: FL2-A
R
TMRE^high cells (%)
NS
shLuc.
shIMPA1
shLuc.
shIMPA1
WT
AMPK-/-
S
WT
AMPK-/-
shLuc.
shIMPA1
shLuc.
shIMPA1
IMPA1
AMPKα
pAMPKα
GAPDH

Figure S5

Figure S5. IMPA1/Inositol regulates mitochondrial respiration and inositol decline upon IMPA1 loss induces decrease of mitochondrial membrane potential in an AMPK-dependent manner, Related to Figure 3 and 4.

(A and B) Mitochondrial membrane potential (ΔΨm) in DU145 or PC3 cells stably expressing shLuc. or shIMPA1 incubated with Tetramethylrhodamine ethyl ester perchlorate (TMRM) was determined by flow cytometry analysis. (C) ΔΨm in DU145 scramble (Scram.) or IMPA1 knockout by CRISPR/Cas9 cells upon indicated plasmid overexpression was determined by flow cytometry analysis. (D) Oxygen consumption rate (OCR) was determined by Seahorse Mito Stress analysis. The PC3 cells stably expressing shLuc. or shIMPA1 upon vehicle or Ins treatment and exposed to oligomycin, FCCP and rotenone/antimycin A. OCR was measure as pmole O_2/min/15000 cells. (E) Immunoblotting of LC3 expression in PC3 cells stably expressing shLuc. or IMPA1 upon vehicle or inositol treatment. (F and G) Quantification of mitochondrial ROS levels in DU145 or PC3 cells stably transduced with shLuc. or shIMPA1 by flow cytometry. NS, non-significant. (H) Cell survival was analyzed by MTT assay (I) Cell growth in shLuc. or shIMPA1 PC3 cells was determined by cell counting using trypan blue. (J) ΔΨm in DU145 cells stably expressing shLuc. or shIMPA1 upon vehicle (Veh.) or 10 μM of Compound C (Comp. C) treatment was determined by flow cytometry analysis. (K) The percentage cells with $TMRM^{high}$, defined by the gate shown in (A and B) in (J) was quantified by flow cytometry analysis. (L) Immunoblotting of DU145 cells stably expressing shLuc. or shIMPA1 upon Veh or Comp. C treatment. (M) ΔΨm in PC3 cells stably expressing shLuc., shIMPA1 #1, shIMPA1 #2 or shAMPKα #1 was determined by flow cytometry analysis. (N) The percentage cells with $TMRM^{high}$ in (M) was quantified by flow cytometry analysis. (O) Immunoblotting of PC3 cells stably expressing shLuc., shIMPA1 #1, shIMPA1 #2 or shAMPKα #1. (P and Q) ΔΨm in wild type MEFs or $AMPK^{-/-}$ MEFs stably expressing shLuc. or shIMPA1 #1. (R) The percentage cells with $TMRM^{high}$ in (P and Q) was quantified by flow cytometry analysis. (S) Immunoblotting of wild type MEFs or $AMPK^{-/-}$ MEFs stably expressing shLuc. or shIMPA1 #1.

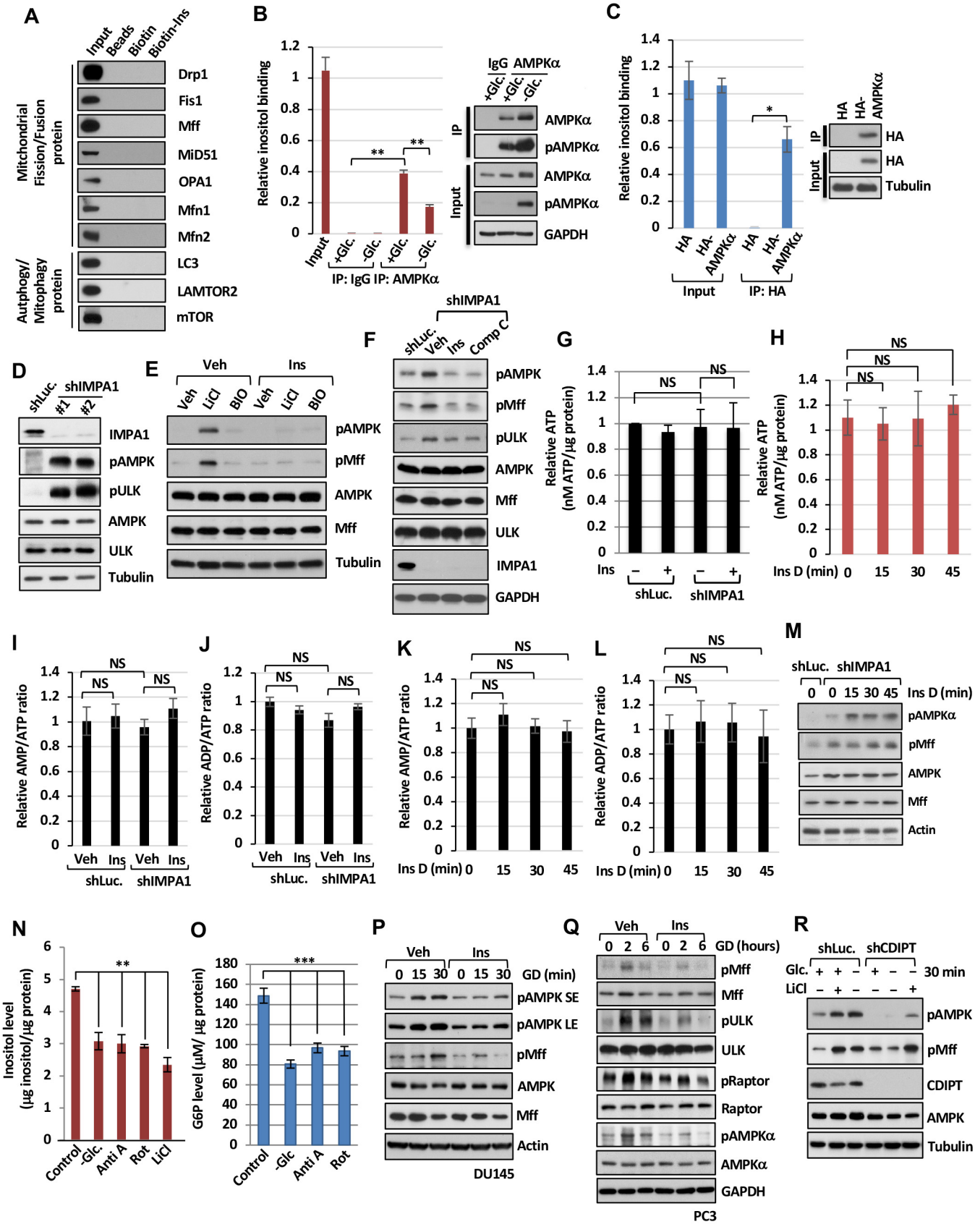
A
Input
Beads
Biotin
Biotin-Ins
Mitchondrial Fission/Fusion protein
Drp1
Fis1
Mff
MiD51
OPA1
Mfn1
Mfn2
Autphogy/ Mitophagy protein
LC3
LAMTOR2
mTOR
B
Relative inositol binding
IgG
AMPKα
+Glc.
-Glc.
IP
Input
AMPKα
pAMPKα
GAPDH
IP: IgG IP: AMPKα
C
Relative inositol binding
HA
HA-AMPKα
Input
IP: HA
Tubulin
D
shLuc.
shIMPA1
#1
#2
IMPA1
pAMPK
pULK
AMPK
ULK
Tubulin
E
Veh
Ins
LiCl
BIO
pAMPK
pMff
AMPK
Mff
Tubulin
F
shIMPA1
Comp C
pAMPK
pMff
pULK
AMPK
Mff
ULK
IMPA1
GAPDH
G
Relative ATP (nM ATP/μg protein)
NS
shLuc.
shIMPA1
H
Ins D (min)
I
Relative AMP/ATP ratio
J
Relative ADP/ATP ratio
K
L
M
Actin
N
Inositol level (μg inositol/μg protein)
Control
-Glc.
Anti A
Rot
LiCl
O
G6P level (μM/ μg protein)
P
GD (min)
pAMPK SE
pAMPK LE
DU145
Q
GD (hours)
pRaptor
Raptor
PC3
R
shCDIPT
Glc.
LiCl
30 min
CDIPT

Figure S6

Figure S6. Inositol decline promotes AMPK activation and mitochondrial fission upon stress conditions, Related to Figure 5. (A) 40 μM of Biotin or Biotin-Ins pulled down and subjected to immunoblotting in PC3 cells. (B) PC3 cells cultured in medium containing 25 mM glucose (+Glc.) or no glucose (-Glc.) were immunoprecipitated with IgG or AMPKα, followed by the elution of metabolites with 80% methanol. The amount of inositol was determined. Immunoprecipitation efficacy was examined by immunoblotting with indicated antibodies. (C) The amount of inositol in HA or HA-AMPKα PC3 cells was determined. (D) Immunoblotting of DU145 cells stably expressing shLuc. or shIMPA1. (E) Immunoblotting of PC3 cells upon 500 μM of lithium chloride, 10 μM of BIO treatment or in combination with Ins treatment. (F) Immunoblotting of shLuc. or shIMPA1 in PC3 cells with vehicle (Veh), Ins or Comp C treatment. (G) The ATP levels in DU145 cells expressing shLuc. or shIMPA1 upon with or without Ins treatment were determined. NS, non-significant. (H) The ATP levels in MEFs upon inositol (Ins) deprivation were determined. (I and J) Metabolic profiling of AMP/ATP and ADP/ATP ratio in DU145 cells expressing shLuc. or shIMPA1 upon vehicle (Veh) or Ins treatment were performed by targeted mass spectrometry analysis. (K and L) Metabolic profiling of AMP/ATP and ADP/ATP ratio in MEFs upon Ins deprivation were performed. (M) Immunoblotting of MEFs stably expressing shLuc. or shIMPA1 upon Ins deprivation (Ins D) (N) The levels of inositol in DU145 cells upon vehicle (control), glucose deprivation (-Glc.), 10 μM of antimycin A (Anti A), 250 ng/ml of rotenone (Rot) or 500 μM of LiCl is determined. (O) The levels of G6P in DU145 cells upon vehicle (control), -Glc., Anti A or Rot treatment is determined by G6P colorimetric assay kit. (P and Q) Immunoblotting of DU145 or PC3 cells upon glucose deprivation (GD) with or without Ins treatment for various times. (R) Immunoblotting of PC3 cells stably expressing shLuc. or shCDIPT upon glucose deprivation or 500 μM of lithium chloride treatment.

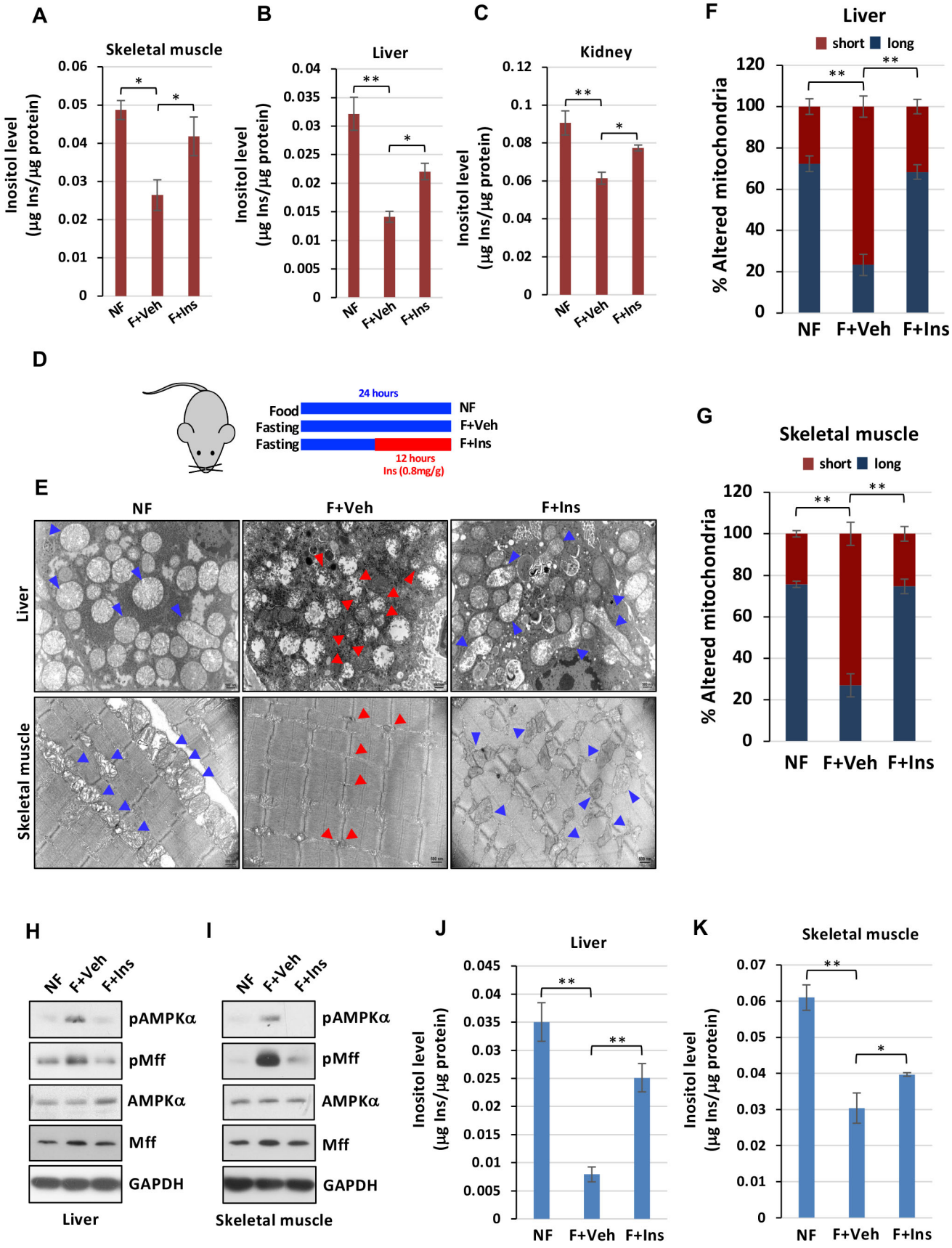
A
Skeletal muscle
Inositol level (μg Ins/μg protein)
NF
F+Veh
F+Ins
B
Liver
C
Kidney
F
Liver
short
long
% Altered mitochondria
D
24 hours
Food
Fasting
Fasting
NF
F+Veh
F+Ins
12 hours
Ins (0.8mg/g)
E
Liver
Skeletal muscle
G
Skeletal muscle
H
pAMPKα
pMff
AMPKα
Mff
GAPDH
Liver
I
Skeletal muscle
J
Liver
K
Skeletal muscle

Figure S7

Figure S7. Inositol decline leads to AMPK activation and mitochondrial fission in fasted mice, Related to Figure 5. (A-C) mice fasted for 24 hours and inositol (Ins) treatment by intraperitoneal injection (IP) at the time point mice fasted for 18 hours. The levels of inositol in tibialis anterior, liver and kidney of mice fed with food, no fasting (NF), fasted with vehicle (F+Veh) or fasted with Ins (F+Ins) was determined. Three male mice were analyzed in each group. (D) The graphic shows mice fasted for 12 hours followed by oral administration of vehicle or Ins by drinking water (0.8 mg/g) for 12 hours under fasting conditions. (E) Representative images of transmission electron microscope upon mice fed with food, no fasting (NF), fasted with vehicle (F+Veh) and fasted with Ins (0.8 mg/g) by drinking water (F+Ins). Blue arrow, healthy/elongated mitochondria; Red arrows, fragmented mitochondria. Scale bar, 500 nm. (F and G) Quantification of the mitochondrial morphology (long and short) shown in (E). (H and I) The proteins extracted from tissues of liver and skeletal muscle (from tibialis anterior) were subjected to Immunoblotting. (J and K) mice fasted for 12 hours, followed by oral administration of vehicle or Ins by drinking water (0.8 mg/g) for 12 hours under fasting conditions. Ins was delivered via water to mice at the dose of 0.8 mg/g of body weight. The levels of Ins in liver and tibialis anterior of mice fed with food, no fasting (NF), fasted with vehicle (F+Veh) or fasted with Ins (F+Ins) were determined.

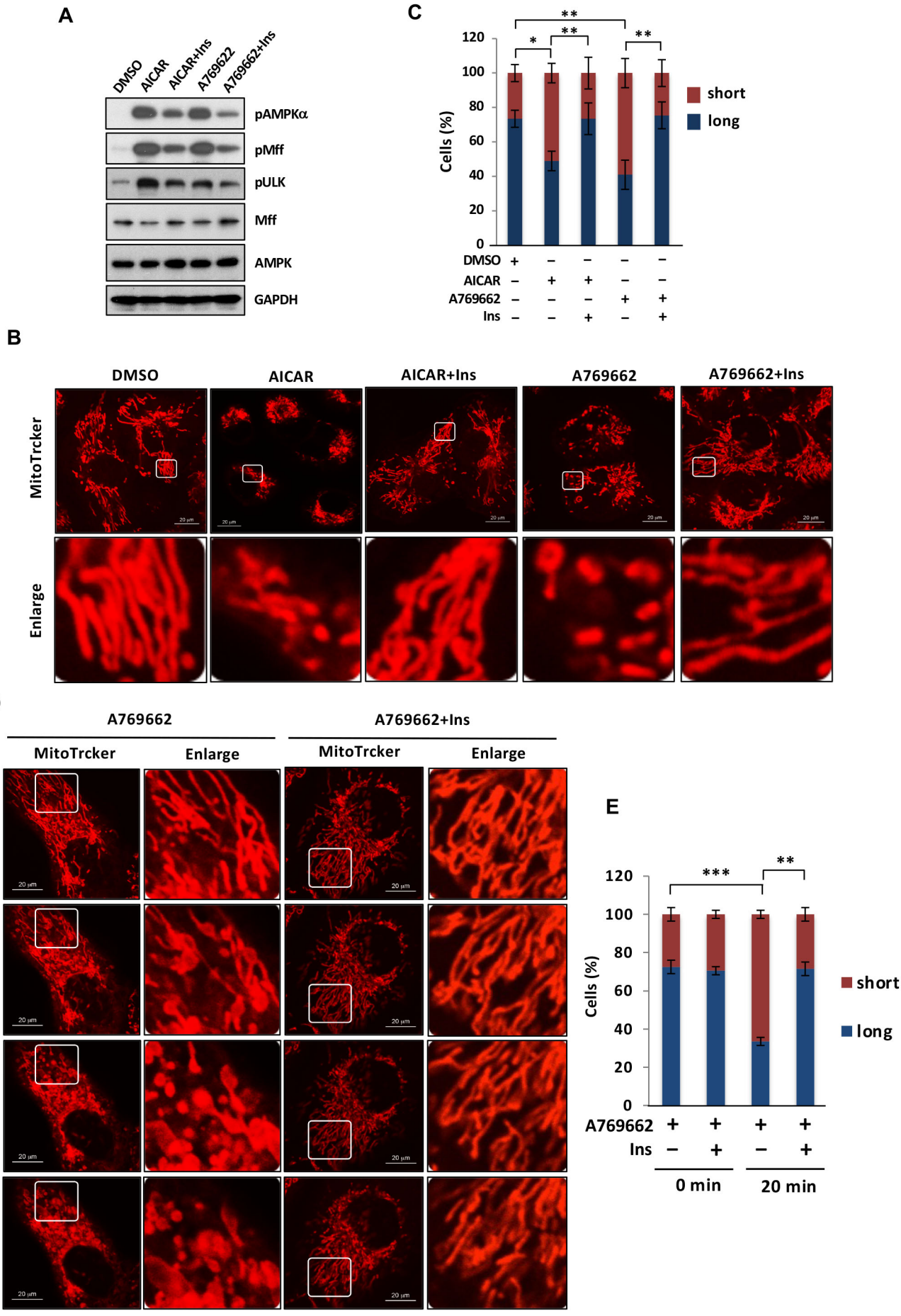
A
DMSO
AICAR
AICAR+Ins
A769662
A769662+Ins
pAMPKα
pMff
pULK
Mff
AMPK
GAPDH
C
Cells (%)
short
long
DMSO
AICAR
A769662
Ins
B
DMSO
AICAR
AICAR+Ins
A769662
A769662+Ins
MitoTrcker
Enlarge
D
A769662
A769662+Ins
MitoTrcker
Enlarge
0 min
5 min
10 min
20 min
E
Cells (%)
short
long
A769662
Ins
0 min
20 min

Figure S8

Figure S8. Inositol inhibits mitochondrial fission induced by various AMPK activators, Related Figure 6. (A) Immunoblotting of PC3 cells upon DMSO, 2 mM of AICAR, 300 μM of A769662 with or without 25 μM of Ins treatment for 1 hour. (B) Representative confocal images in DU145 cells upon DMSO, 2 mM of AICAR, 300 μM of A769662 with or without 25 μM of Ins treatment for 1 hour. Scale bar, 20 μm. (C) Quantification of the mitochondrial morphology of the cells shown in (B). Colors indicate the mitochondrial morphology (long or short). (D) Time-lapse images of DU145 cells stained with MitoTracker Red FM (red) upon A769662 with or without Ins treatment. A magnification of a portion of mitochondria was included for each image. Scale bar, 20 μm. (E) Quantification of the mitochondrial morphology of the cells shown in (D) at 0 min or 20 min. Colors indicate the mitochondrial morphology (long or short). Representative immunoblotting blots for each dataset were presented from at least three times of the repeated experiments.

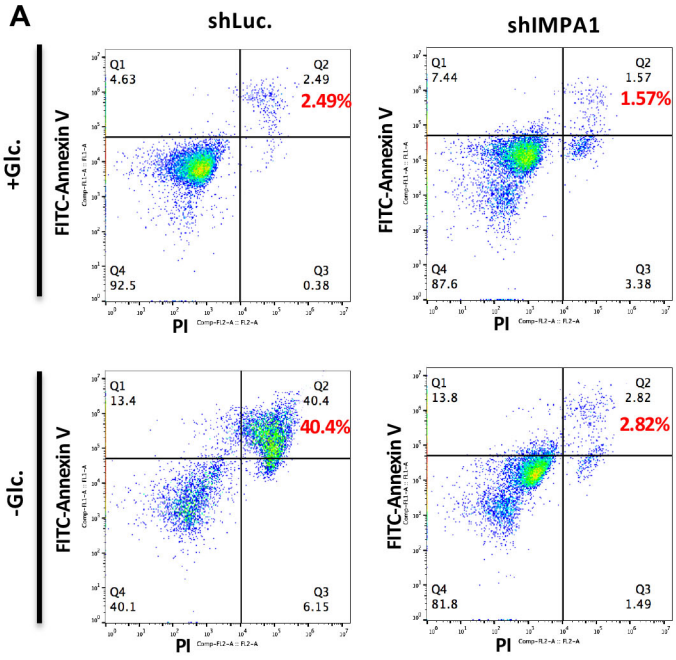
A
shLuc.
shIMPA1
+Glc.
-Glc.
FITC-Annexin V
PI
Q1
4.63
Q2
2.49
2.49%
Q4
92.5
Q3
0.38
Q1
7.44
Q2
1.57
1.57%
Q4
87.6
Q3
3.38
Q1
13.4
Q2
40.4
40.4%
Q4
40.1
Q3
6.15
Q1
13.8
Q2
2.82
2.82%
Q4
81.8
Q3
1.49

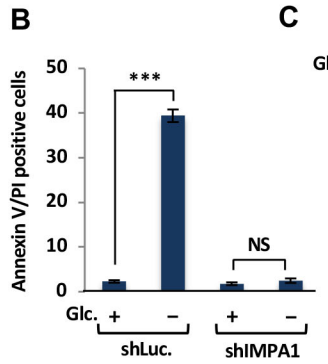
B
Annexin V/PI positive cells
50
40
30
20
10
0
***
NS
Glc.
+
–
+
–
shLuc.
shIMPA1

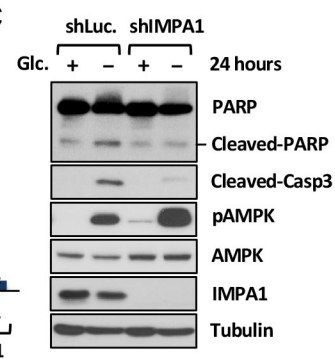
C
shLuc.
shIMPA1
Glc.
+
–
+
–
24 hours
PARP
Cleaved-PARP
Cleaved-Casp3
pAMPK
AMPK
IMPA1
Tubulin

Figure S9

Figure S9. IMPA1 regulates AMPK activity and cell survival upon glucose deprivation, Related to Figure 6. (A) The MEFs stably expressing shLuc. or shIMPA1 upon glucose deprivation (-Glc.) for 24 hours were incubated with Annexin V-FITC and propidium iodide (PI), followed by flow cytometry analysis. (B) Quantification of Annexin V/PI-positive cells by flow cytometry. (C) Immunoblotting of MEFs stably expressing shLuc. or shIMPA1 upon glucose deprivation for 24 hours. Representative immunoblotting blots for each dataset were presented from at least three times of the repeated experiments.

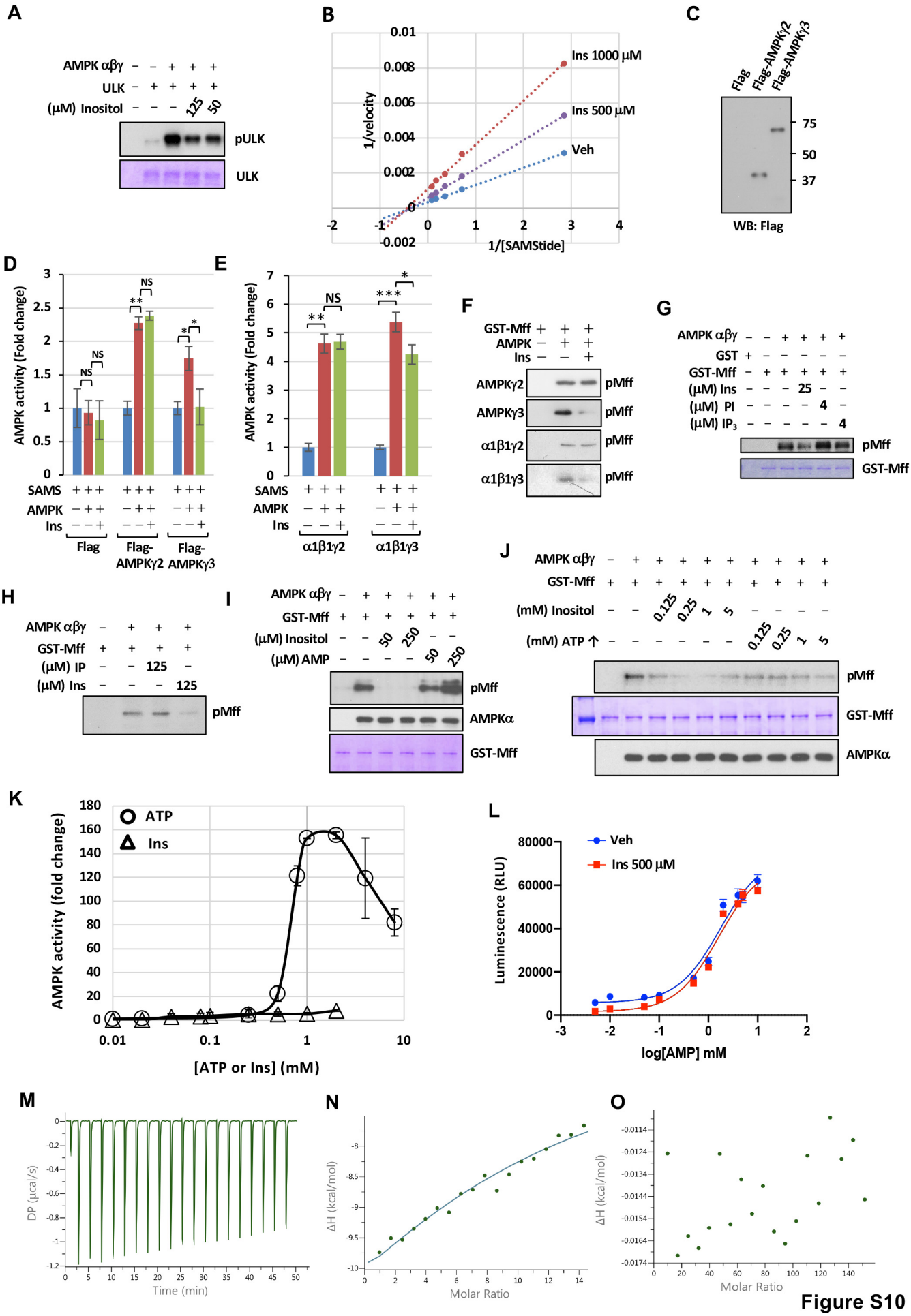
A
AMPK αβγ
ULK
(μM) Inositol
125
50
pULK
ULK
B
1/velocity
1/[SAMStide]
Ins 1000 μM
Ins 500 μM
Veh
C
Flag
Flag-AMPKγ2
Flag-AMPKγ3
75
50
37
WB: Flag
D
AMPK activity (Fold change)
NS
SAMS
AMPK
Ins
Flag
Flag-AMPKγ2
Flag-AMPKγ3
E
AMPK activity (Fold change)
α1β1γ2
α1β1γ3
F
GST-Mff
AMPK
Ins
AMPKγ2
AMPKγ3
α1β1γ2
α1β1γ3
pMff
G
AMPK αβγ
GST
GST-Mff
(μM) Ins
(μM) PI
(μM) IP3
pMff
GST-Mff
H
AMPK αβγ
GST-Mff
(μM) IP
(μM) Ins
pMff
I
AMPK αβγ
GST-Mff
(μM) Inositol
(μM) AMP
pMff
AMPKα
GST-Mff
J
AMPK αβγ
GST-Mff
(mM) Inositol
(mM) ATP
pMff
GST-Mff
AMPKα
K
AMPK activity (fold change)
ATP
Ins
[ATP or Ins] (mM)
L
Luminescence (RLU)
Veh
Ins 500 μM
log[AMP] mM
M
DP (μcal/s)
Time (min)
N
ΔH (kcal/mol)
Molar Ratio
O
ΔH (kcal/mol)
Molar Ratio

Figure S10

Figure S10. Inositol inhibits AMPK complex activity and directly binds to AMPKγ subunit, Related to Figure 7. (A) AMPK kinase activity with fixed amount of ATP (0.5 mM) was determined by immunoblotting with phospho-ULK S555 antibody. (B) Linweaver-Burk plot for non-competitive inhibition of inositol on AMPK-catalyzed SAMS peptide phosphorylation was determined by using 1/velocity of Michaelis-Menten curve plot versus 1/the concentration of SAMS peptide. (C) Immunoblotting of purified proteins of Flag vector control, Flag-AMPKγ2 and Flag-AMPKγ3 with Flag antibody. (D) Flag vector control, Flag-AMPKγ2 and Flag-AMPKγ3 complexes kinase activity was determined by ADP-Glo^{TM} kinase assay (E) Diverse AMPK complex kinase activity was determined by ADP-Glo^{TM} kinase assay. (F) Diverse AMPK complexes kinase activity was determined by immunoblotting with phospho-Mff S146 antibody. (G) AMPK kinase activity upon 25 μM of Ins, 4 μM of PI or IP_3 incubation was determined by immunoblotting with phospho-Mff S146 antibody. (H) AMPK kinase activity by adding IP or Ins was determined by immunoblotting with phospho-Mff S146 antibody. (I) AMPK kinase activity by adding inositol or AMP was determined by immunoblotting with phospho-Mff S146 antibody. (J) AMPK kinase activity by adding Ins or ATP was determined by immunoblotting with phospho-Mff S146 antibody. (K) AMPK enzymatic activity curve (fold change) in response to ATP or Ins concentrations using SAMS peptide phosphorylation assay. Data were fitted to the equation $Y = \text{basal} + \{[(\text{activation} \times \text{basal} - \text{basal}) \times X] / (EC_{50} + X)\}$ and then normalized with basal, where Y is kinase activity and X is ATP or Ins concentrations. (L) AMPK enzymatic activity curve (RLU, relative light units) in response to AMP concentrations with or without inositol (500 μM) using SAMS peptide phosphorylation assay. (M and N) The binding between inositol and GST-AMPKγ was determined by isothermal titration calorimetry (ITC) assay with dissociation constant (K_d) of 469 μM. (O) The binding between inositol and GST was determined by isothermal titration calorimetry (ITC) assay as a control to rule out non-specific binding.

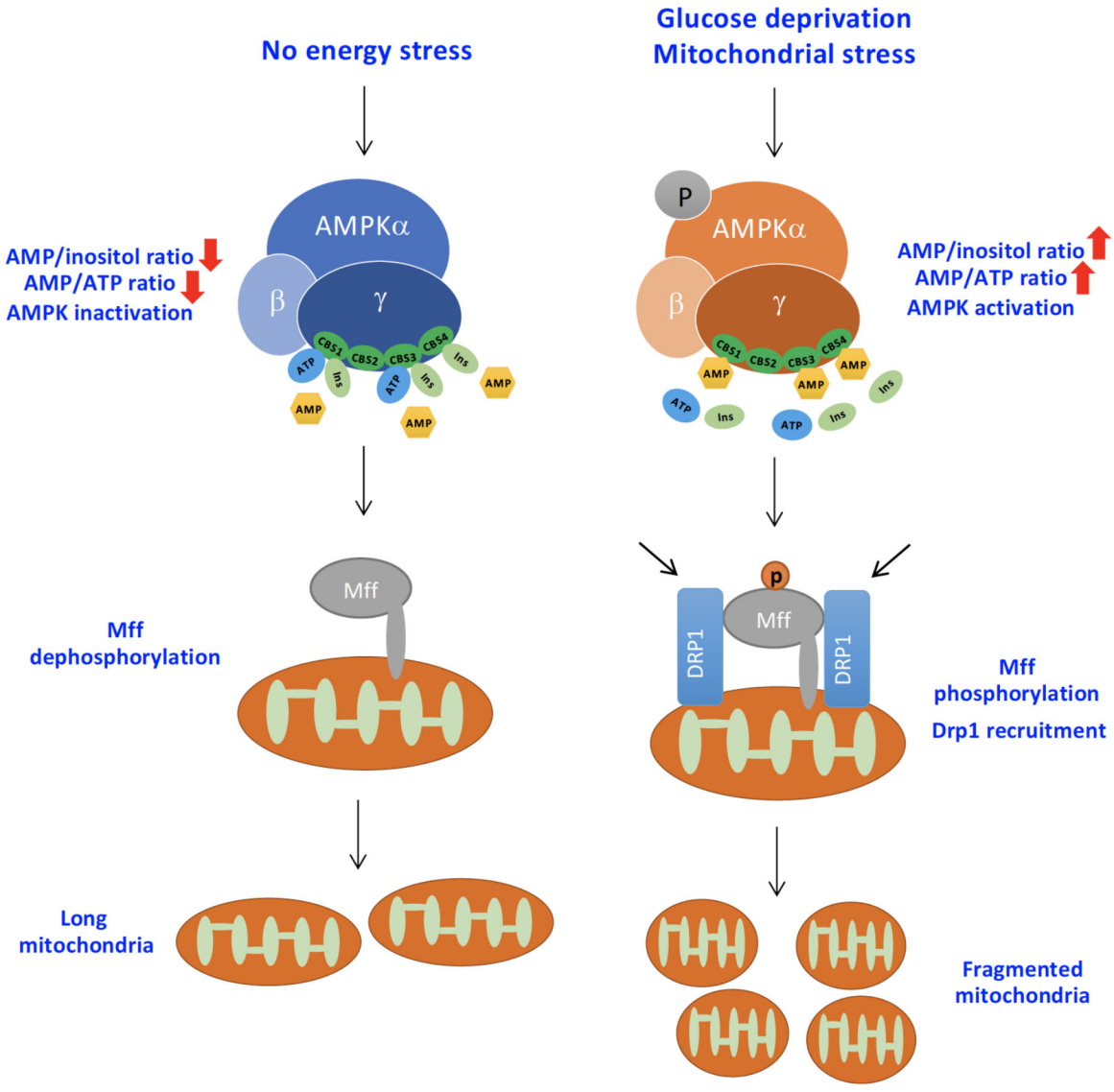
No energy stress
Glucose deprivation
Mitochondrial stress
AMPKα
β
γ
P
CBS1
CBS2
CBS3
CBS4
ATP
Ins
AMP
AMP/inositol ratio
AMP/ATP ratio
AMPK inactivation
AMP/inositol ratio
AMP/ATP ratio
AMPK activation
Mff
p
DRP1
Mff dephosphorylation
Mff phosphorylation
Drp1 recruitment
Long mitochondria
Fragmented mitochondria

Figure S11

Figure S11. Working model for inositol in restricting AMPK activation and mitochondrial fission, Related to Figure 5, 6 and 7. Inositol serves as an endogenous suppressor to limit AMPK activation and mitochondrial fission through its binding to the AMPKγ subunit. In normal physiological conditions without energy stress, inositol and ATP levels are high and both inositol and ATP bind to AMPKγ to repress AMPK activity and mitochondrial fission; however, under energy stresses or bioenergetic failure such as glucose deprivation and mitochondrial damage, inositol and ATP levels decline, accompanied with the increase in AMP level, hence allowing for AMP binding to AMPKγ subunit to induce AMPK activation and subsequent mitochondrial fission. This model suggests that both AMP/inositol and AMP/ATP ratio serve as critical determinants for AMPK activation and mitochondrial fission, offering the molecular insight into how metabolic stress drives AMPK activation. AMPK is therefore an inositol sensor orchestrating mitochondrial fission by detecting the inositol gradient in cells.